Green-function theory of the Heisenberg ferromagnet in a magnetic field

I. Junger and D. Ihle

Institut für Theoretische Physik, Universität Leipzig, D-04109 Leipzig, Germany

J. Richter

Institut für Theoretische Physik, Otto-von-Guericke-Universität Magdeburg, D-39016 Magdeburg, Germany

A. Klümper

Theoretische Physik, Bergische Universität Wuppertal, D-42097 Wuppertal, Germany

We present a second-order Green-function theory of the one- and two-dimensional $S=1/2$ ferromagnet in a magnetic field based on a decoupling of three-spin operator products, where vertex parameters are introduced and determined by exact relations. The transverse and longitudinal spin correlation functions and thermodynamic properties (magnetization, isothermal magnetic susceptibility, specific heat) are calculated self-consistently at arbitrary temperatures and fields. In addition, exact diagonalizations on finite lattices and, in the one-dimensional case, exact calculations by the Bethe-ansatz method for the quantum transfer matrix are performed. A good agreement of the Green-function theory with the exact data, with recent quantum Monte Carlo results, and with the spin polarization of a $\nu=1$ quantum Hall ferromagnet is obtained. The field dependences of the position and height of the maximum in the temperature dependence of the susceptibility are found to fit well to power laws, which are critically analyzed in relation to the recently discussed behavior in Landau's theory. As revealed by the spin correlation functions and the specific heat at low fields, our theory provides an improved description of magnetic short-range order as compared with the random phase approximation. In one dimension and at very low fields, two maxima in the temperature dependence of the specific heat are found. The Bethe-ansatz data for the field dependences of the position and height of the low-temperature maximum are described by power laws. At higher fields in one and two dimensions, the temperature of the specific heat maximum linearly increases with the field.

I. INTRODUCTION

In the theory of low-dimensional magnetism the essential role of quantum and thermal fluctuations, especially in the description of magnetic short-range order (SRO) at arbitrary temperatures, is of basic interest. Whereas for Heisenberg antiferromagnets the interplay of low dimensionality and quantum fluctuations is important already at $T=0$, in ferromagnets quantum fluctuations occur at nonzero temperatures only. The study of low-dimensional quantum ferromagnets in a magnetic field was motivated by the progress in the synthesis of materials, such as the $\nu=1$ quantum Hall ferromagnets,[1] which may be described by an effective two-dimensional (2D) $S=1/2$ Heisenberg model,[2–4] the quasi-2D ferromagnetic insulators A_2CuF_4 (A=K, Cs),[5,6] La_2BaCuO_5,[5] and Rb_2CrCl_4,[7] the quasi-1D organic ferromagnet p-NPNN $(C_{13}H_{16}N_3O_4)$,[8] and the quasi-1D copper salt $TMCuC[(CH_3)_4NCuCl_3]$.[9]

The 2D $S=1/2$ ferromagnet in a field was investigated by Green-function decouplings of first order,[10] i.e., by the random phase approximation (RPA)[11] and the Callen decoupling,[12] by Schwinger boson theories,[2,3] and by quantum Monte Carlo (QMC) simulations.[3,4] Thereby, the magnetization[2–4,10] and the spin lattice relaxation rate[2,4] were calculated. The 1D ferromagnet was studied by the Bethe-ansatz method, where some exact data for the zero-field magnetic susceptibility and specific heat[13] as well as for the mag-

netization and correlation length were given.[14] Recently, in the 1D model a power law for the shift of the temperature of the susceptibility maximum with the field was reported and argued from Landau's theory to appear in the 2D model, too.[15] Therefore, a detailed analysis of the thermodynamic quantities of the 1D and 2D Heisenberg ferromagnets as functions of temperature and field is of interest, also for comparison with experiments.

We consider the $S=1/2$ Heisenberg model

$$H = -\frac{J}{2}\sum_{\langle i,j\rangle} \mathbf{S}_i \mathbf{S}_j - h\sum_i S_i^z. \qquad (1)$$

[$\langle i,j\rangle$ denote nearest-neighbor (NN) sites; throughout we set $J=1$] along a chain and on a square lattice. To provide an improved description of SRO and of the thermodynamics (magnetization, magnetic susceptibility, specific heat) as compared with the standard approaches,[10] we go one step beyond the first-order Green-function decouplings. To this end, we adapt the Green-function projection method dealing with second time derivatives of spin operators outlined in Refs. 16 and 17. Furthermore, we perform exact finite-lattice diagonalizations (ED) on a $N=16$ chain and a $N=4\times4$ square lattice using periodic boundary conditions.

The exact Bethe-ansatz results for the 1D case are obtained from an eigenvalue analysis of the quantum transfer matrix of the Heisenberg chain, a concept that is also the

basis of the work reported in Ref. 14. Here, unlike the treatment in Ref. 14, we perform this analysis by solving a certain set of nonlinear integral equations to be found for instance in Ref. 18. These integral equations were analyzed in the literature extensively for the antiferromagnetic Heisenberg chain. The ferromagnetic case satisfies the same set of equations with just a sign change in the temperature dependent term. Despite this rather minor change in the analytical formulation the numerical treatment of these equations is rather different from the antiferromagnetic case. The iterative treatment is plagued by slow convergence, in particular for low fields and low temperatures. A numerically much better conditioned formulation can be derived by combining the methods of Refs. 18 and 19. Details of these calculations will be given elsewhere. Our results are in perfect agreement with those of Refs. 13 and 14 if available.

II. GREEN-FUNCTION THEORY

To calculate the transverse and longitudinal spin correlation functions we determine the two-time retarded commutator Green functions $G_q^{\nu\mu}(\omega)=\langle\langle S_q^\nu;S_{-q}^\mu\rangle\rangle_\omega$ $(\nu\mu=+-,zz)$ by the projection method, where we neglect the self-energy.[16,17] Taking into account the breaking of spin-rotational symmetry by the magnetic field we choose, as for the XXZ model,[17] the two-operator basis $(S_q^+,i\dot{S}_q^+)$ and $(S_q^z,i\dot{S}_q^z)$. To approximate the time evolution of the spin operators $-\ddot{S}_q^+$ and $-\ddot{S}_q^z$, we take the site representation and decouple the products of three spin operators in $-\ddot{S}_i^+$ and $-\ddot{S}_i^z$ along NN sequences $\langle i,j,l\rangle$ introducing vertex parameters $\alpha^{\nu\mu}$ in the spirit of the scheme proposed in Refs. 17 and 20,

$$S_i^+S_j^+S_l^- = \alpha^{+-}\langle S_j^+S_l^-\rangle S_i^+ + \alpha^{+-}\langle S_i^+S_l^-\rangle S_j^+, \quad (2)$$

$$S_i^zS_j^+S_l^- = \alpha^{zz}\langle S_j^+S_l^-\rangle S_i^z. \quad (3)$$

Here, following the investigation of the ferromagnet at $h=0$,[20] the dependence on the relative site positions of the vertex parameters (cf. Ref. 16) is neglected. We obtain

$$-\ddot{S}_q^+ = [(\omega_q^{+-})^2 - h^2]S_q^+ + 2hi\dot{S}_q^+, \quad (4)$$

$$-\ddot{S}_q^z = (\omega_q^{zz})^2S_q^z, \quad (5)$$

with

$$(\omega_q^{+-})^2 = \frac{z}{2}(1-\gamma_q)\{\Delta^{+-} + 2z\alpha^{+-}C_{10}(1-\gamma_q)\}, \quad (6)$$

$$\Delta^{+-} = 1 + 2\alpha^{+-}\{(z-2)C_{11} + C_{20} - (z+1)C_{10}\}; \quad (7)$$

$$(\omega_q^{zz})^2 = \frac{z}{2}(1-\gamma_q)\{\Delta^{zz} + 2z\alpha^{zz}C_{10}^{+-}(1-\gamma_q)\}, \quad (8)$$

$$\Delta^{zz} = 1 + 2\alpha^{zz}\{(z-2)C_{11}^{+-} + C_{20}^{+-} - (z+1)C_{10}^{+-}\}, \quad (9)$$

where $C_{nm}=\frac{1}{2}C_{nm}^{+-}+C_{nm}^{zz}$, $C_{nm}^{\mu\nu}\equiv C_R^{\mu\nu}=\langle S_0^\mu S_R^\nu\rangle$, $R=ne_x+me_y$, $\gamma_q=\frac{2}{z}\Sigma_{i=1}^{z/2}\cos q_i$, and z is the coordination number. This ap-

proximation, Eqs. (4) and (5), is equivalent to the equation of motion decoupling in second order.[20] Finally, we obtain

$$G_q^{+-}(\omega) = \sum_{i=1,2}\frac{A_{qi}}{\omega-\omega_{qi}}; \quad \omega_{q1,2}=h\pm\omega_q^{+-}, \quad (10)$$

$$G_q^{zz}(\omega) = \frac{M_q^{zz}}{\omega^2 - (\omega_q^{zz})^2}, \quad (11)$$

with

$$A_{q1,2} = \langle S^z\rangle \pm \frac{1}{2\omega_q^{+-}}(M_q^{+-} - 2h\langle S^z\rangle). \quad (12)$$

The first spectral moments $M_q^{+-}=\langle[i\dot{S}_q^+,S_{-q}^-]\rangle$ and $M_q^{zz}=\langle[i\dot{S}_q^z,S_{-q}^z]\rangle$ are given by the exact expressions

$$M_q^{+-} = 2zC_{10}(1-\gamma_q) + 2h\langle S^z\rangle, \quad (13)$$

$$M_q^{zz} = zC_{10}^{+-}(1-\gamma_q). \quad (14)$$

The spin correlators are calculated as $C_R^{\mu\nu}=\frac{1}{N}\Sigma_q C_q^{\mu\nu}e^{iqR}$ with $C_q^{\mu\nu}=\langle S_q^\mu S_{-q}^\nu\rangle$. By Eqs. (10) and (11) we get

$$C_q^{-+} = \sum_{i=1,2} A_{qi}n(\omega_{qi}), \quad C_q^{zz} = \tilde{C}_q^{zz} + D_q^{zz}, \quad (15)$$

$$\tilde{C}_q^{zz} = \frac{M_q^{zz}}{2\omega_q^{zz}}[1 + 2n(\omega_q^{zz})], \quad (16)$$

where $n(\omega)=(e^{\omega/T}-1)^{-1}$. As shown in Ref. 21, for the complete determination of correlation functions calculated from commutator Green functions one has to take into account an additional term, if the corresponding anticommutator Green function has a pole at $\omega=0$. Here, we have[21]

$$D_q^{zz} = \lim_{\omega\to 0}\frac{\omega}{2}G_q^{(+)zz}(\omega). \quad (17)$$

The equation of motion for the anticommutator Green function $G_q^{(+)zz}(\omega)$ yields Eq. (11) with M_q^{zz} replaced by $M_q^{(+)zz} + 2\omega C_q^{zz}$, where $M_q^{(+)zz}=\langle[i\dot{S}_q^z,S_{-q}^z]_+\rangle$. By the spectral theorem for C_q^{zz} it can be easily verified that $M_q^{(+)zz}=0$. Thus, Eq. (17) with $\omega_{q=0}^{zz}=0$ yields

$$D_q^{zz} = C_q^{zz}\delta_{q,0} = \sum_R C_R^{zz}\delta_{q,0}. \quad (18)$$

From Eqs. (15) and (18) we have $\tilde{C}_{q=0}^{zz}=0$. By the relation

$$\frac{1}{N}\frac{\partial\langle S^z\rangle}{\partial h} = \frac{1}{T}\left(\frac{1}{N}\sum_R C_R^{zz} - \langle S^z\rangle^2\right), \quad (19)$$

following from the first and second derivatives of the partition function with respect to h, in the thermodynamic limit we finally obtain

$$C_R^{zz} = \frac{1}{N}\sum_{q(\neq 0)}\tilde{C}_q^{zz}e^{iqR} + \langle S^z\rangle^2. \quad (20)$$

Note that the transverse correlator has no additional term, i.e., $D_q^{-+}=0$, because of $\omega_{q=0;1,2}=h\neq 0$.

The magnetization per site, $m = -2\mu_B \langle S^z \rangle$, is calculated as

$$\langle S^z \rangle = \frac{1}{2} - C_0^{-+}. \qquad (21)$$

From $\langle S^z \rangle$ the isothermal magnetic susceptibility $\chi = 4\mu_B^2 \chi_S$ with $\chi_S = \partial \langle S^z \rangle / \partial h$ may be derived.

To complete our scheme, the two vertex parameters $\alpha^{\nu\mu}(T,h)$ have to be determined. To this end, we use the sum rule $C_0^{zz} = 1/4$ and the exact representation of the internal energy per site $u = \langle H \rangle / N$ in terms of $G_q^{+-}(\omega)$,[21] i.e.,

$$-\frac{z}{2}(C_{10}^{+-} + C_{10}^{zz}) - h\langle S^z \rangle$$

$$= -\frac{z}{8} - \frac{h}{2} - \frac{1}{2N}\sum_q \int_{-\infty}^{\infty} \frac{d\omega}{2\pi}(\varepsilon_q + \omega)\mathrm{Im}\, G_q^{+-}(\omega)n(\omega),$$
$$(22)$$

where $\varepsilon_q = z(1 - \gamma_q) + h/2$. Thus, we have a closed system of equations for nine quantities $(\langle S^z \rangle, C_{10}^{\mu\nu}, C_{11}^{\mu\nu}, C_{20}^{\mu\nu}, \alpha^{zz}, \alpha^{+-})$ to be determined self-consistently as functions of temperature and field. As may be easily seen, at $T = 0$ the exact results $\langle S^z \rangle = 1/2$, $C_R^{zz} = 1/4$, and $C_R^{-+} = 0$ are reproduced.

In the case $h = 0$ the spin-rotational symmetry, implying $\langle S^z \rangle = 0$ and $C_R^{+-} = 2C_R^{zz}$, is preserved by our scheme with $\alpha^{+-} = \alpha^{zz} \equiv \alpha$, and the theory reduces to that of Refs. 20 and 22.

It is of interest to compare our results with the RPA[11] which employs the decoupling $i\dot{S}_q^+ = \omega_q S_q^+$ and yields

$$G_q^{+-}(\omega) = \frac{2\langle S^z \rangle}{\omega - \omega_q}, \quad \omega_q = z\langle S^z \rangle(1 - \gamma_q) + h, \qquad (23)$$

$$\frac{1}{\langle S^z \rangle} = \frac{2}{N}\sum_q \coth \frac{\omega_q}{2T}. \qquad (24)$$

Note that the longitudinal correlation functions cannot be obtained by such a simple decoupling, except for C_{10}^{zz} which may be calculated in RPA by Eqs. (22) and (23).

At $h = 0$, in Ref. 23 the RPA was extended to the disordered phase, i.e., to $T > 0$ for 1D and 2D ferromagnets (Mermin-Wagner theorem). Introducing the ratio $\lambda = \lim_{h \to 0} h/z\langle S^z \rangle$, by Eq. (24) with $\coth \omega_q/2T = 2T/\omega_q$, λ is calculated from

$$\frac{1}{N}\sum_q \frac{1}{1 - \gamma_q + \lambda} = \frac{z}{4T}. \qquad (25)$$

The zero-field susceptibility is given by $\chi_S(h=0) = (z\lambda)^{-1}$.

III. RESULTS AND DISCUSSION

A. Magnetization

Considering the magnetization of the chain, in Fig. 1(a) the analytical and ED results as well as our Bethe-ansatz solution are plotted and compared with the RPA results. Let us emphasize the excellent agreement of our theory for the
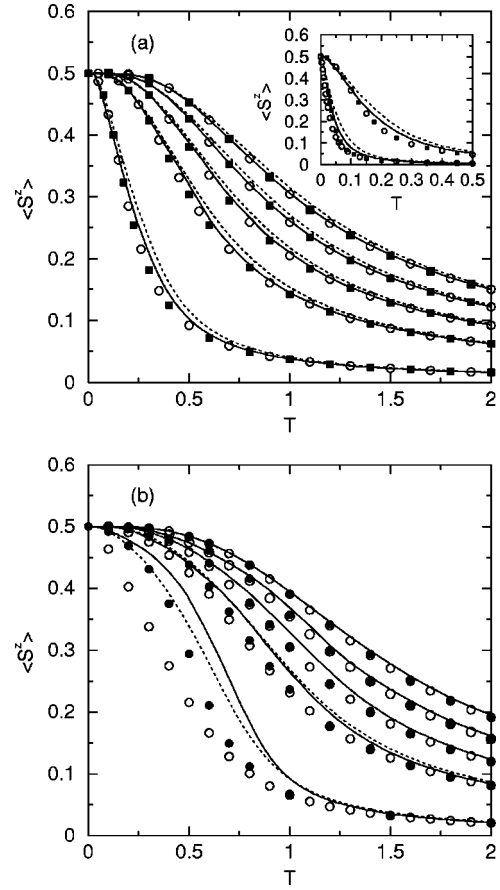

FIG. 1. Magnetization of the 1D (a) and 2D (b) Heisenberg ferromagnet in magnetic fields of strengths $h = 1.0$, 0.8, 0.6, 0.4, and 0.1, from top to bottom, as obtained by the Green-function theory (solid), the ED (○), and the Bethe-ansatz method (■), compared with RPA results (dotted) and QMC data (●, Ref. 4). The inset shows the low-field magnetization of the 1D model at $h = 0.05$ and 0.005 from top to bottom.

chain with the ED and Bethe-ansatz data over the whole temperature and field regions. For the 1D ferromagnet the RPA turns out to be a remarkably good approximation for $\langle S^z \rangle$. In the inset the magnetization at low fields is depicted, since the low-field behavior of the specific heat turned out to be of particular interest (see below). Note that the experimental accessibility to the magnetic field strengths B corresponding to a given h value may be checked from the relation $h = 0.116B[\mathrm{T}]/J[\mathrm{meV}]$. Considering, e.g., the quasi-1D ferromagnet TMCuC with $J = 2.6$ meV,[9] the value $h = 0.05$ corresponds to the magnetic field $B \simeq 1$ T. In Fig. 1(b) our result for the 2D ferromagnet, together with the QMC data for a 32×32 system, are shown. Comparing the ED with the QMC results, the finite-size effects are seen to be largest for low fields and at intermediate temperatures (cf. Ref. 4); for large fields ($h \gtrsim 0.4$) they become small. Furthermore, as can be seen in Fig. 1, the finite-size effects in the 2D model are more pronounced than in the 1D model. This may be due to the smaller linear extension of the 2D system as compared with the chain of an equal number of spins. In two dimensions, at low fields ($h \lesssim 0.3$) the result of our theory is somewhat worse than that of the RPA, although we have included
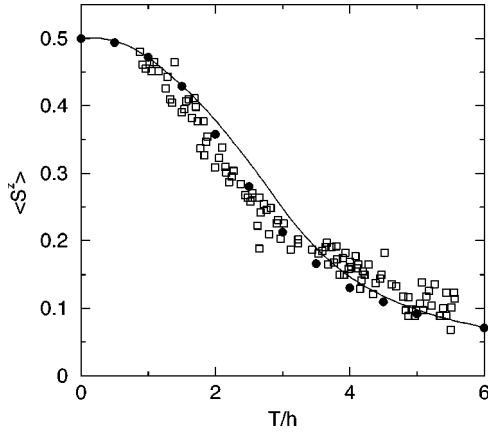
FIG. 2. Magnetization for the $\nu=1$ quantum Hall ferromagnet calculated at $h=0.32$ (solid) in comparison with QMC ($\bullet$, Ref. 4) and experimental data ($\square$, Ref. 1).

additional spin correlations. This behavior is analogous to the results for the magnetization in Ref. 10, where the RPA is found to be closer to the QMC data than the Callen decoupling. For higher fields ($h\gtrsim 0.3$) this tendency is reversed, i.e., our magnetization curves lie slightly below the RPA curves and closer to the QMC data.

Figure 2 shows the spin polarization of a $\nu=1$ quantum Hall ferromagnet measured by magnetoabsorption spectrosocopy[1] in comparison with our theory and QMC data, where $h=0.32$ is taken.[3,4] The very good agreement gives a justification for the use of an effective 2D Heisenberg model to describe this itinerant ferromagnet. This should be further confirmed by the comparison of other thermodynamic quantities (magnetic susceptibility, specific heat) with experimental data which, however, is not yet available.

B. Magnetic susceptibility

Let us consider the isothermal susceptibility $\chi_s = \partial\langle S^z\rangle/\partial h$ shown in Figs. 3 and 4. For $h=0$, χ_s diverges at $T=0$ indicating the ferromagnetic phase transition. In one dimension [see inset of Fig. 3(a)], the Bethe-ansatz result $\lim_{T\to 0}\chi_s T^2=1/24$ (Ref. 13) is reproduced by the spin-rotation-invariant Green-function theory.[22] At low temperatures, the deviation of the ED data, calculated from $\chi_s = T^{-1}\Sigma_R C_R^{zz}$, is ascribed to finite-size effects. Contrary, the RPA curve, obtained by Eq. (25) which yields $\lambda=\sqrt{1+4T^2}$ -1 (Ref. 23), strongly deviates from the exact result. In the 2D system, the zero-field susceptibility (see inset of Fig. 4) of the rotation-invariant theory corrects the numerical values given in Ref. 20 and agrees well with the ED result. At nonzero fields we have $\chi_s(T=0)=0$. Therefore, the susceptibility has a maximum at T_m^χ, where T_m^χ increases and $\chi_s(T_m^\chi)$ decreases with increasing field. In one dimension (Fig. 3), the good agreement between Green-function theory, Bethe-ansatz method, and ED corresponds to the results depicted in Fig. 1(a). The deviation of our theory for the 2D model at $h=0.4$ and $T\lesssim 1$ from the ED data (Fig. 4) is due to finite-size effects in $\langle S^z\rangle$, as can be seen in Fig. 1(b).

Recently, the field dependence of the position of the susceptibility maximum has been discussed in connection with
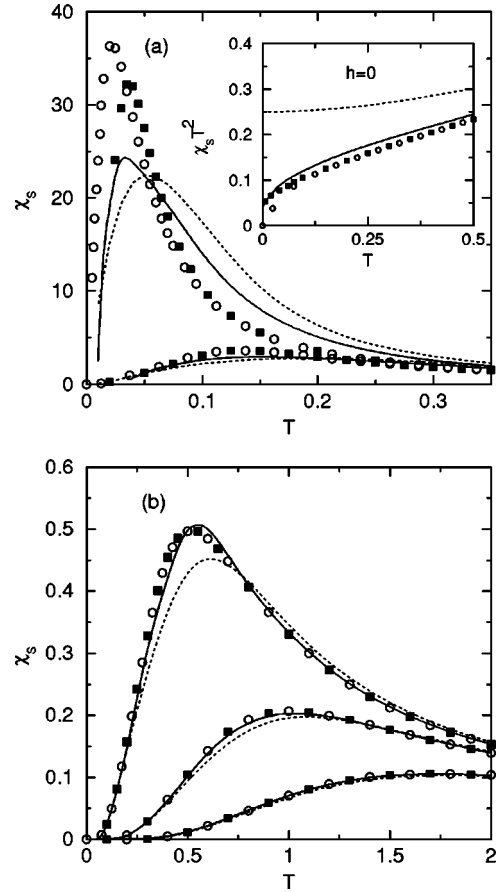

FIG. 3. Isothermal susceptibility of the 1D ferromagnet at low fields (a), $h=0.005$ and 0.05, from top to bottom, and at higher fields (b), $h=0.4$, 1.0, and 2.0, from top to bottom, where the Green-function (solid), ED ($\bigcirc$), Bethe-ansatz ($\blacksquare$), and the RPA results (dotted) are shown. In the inset the 1D zero-field susceptibility is depicted.

experiments on $La_{0.91}Mn_{0.95}O_3$ showing a shift of the maximum in the temperature derivative of the electrical resistivity at an applied field according to $h^{2/3}$ (Ref. 24). Assuming that this maximum coincides with the maximum in the susceptibility due to spin scattering, the dependence $T_m^\chi(h)$ was investigated in terms of Landau's theory, developed for anisotropic systems with $T_c(h=0)\neq 0$, which yields $T_m^\chi\propto h^{2/3}$ (Refs. 15 and 24). Within Landau's theory Sznajd[15] claims that this power law also holds for isotropic ferromagnets in a field. Considering, as a further characteristic, the height of the susceptibility maximum $\chi_s(T_m^\chi)$, Landau's theory[15] yields $\chi_s(T_m^\chi)\propto m^{-2}(T_m^\chi)\propto h^{-2/3}$. In Ref. 15 the isotropic spin chain was investigated by a real-space renormalization group method and $T_m^\chi\propto h^\gamma$ with $\gamma=0.696$ for $0.1<h<5$ was found; however, $\chi_s(T_m^\chi)$ was not calculated.

To analyze the power-law behavior in more detail, the dependence $T_m^\chi(h)$ is plotted logarithmically in Fig. 5(a) for $h\geqslant 0.1$. Both the results of our theory and the ED data for T_m^χ may be well fit to power laws in the 1D (2D) model for $h>0.2$ (0.6). The Green-function theory yields
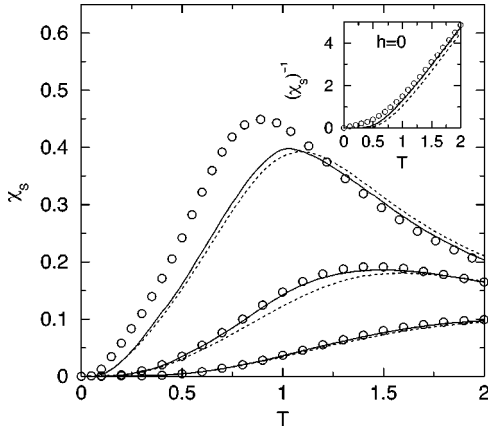
$$T_m^\chi = ah^\gamma \tag{26}$$

with

FIG. 4. Isothermal susceptibility of the 2D ferromagnet at $h=0.4$, 1.0, and 2.0, from top to bottom. The Green-function theory (solid) is compared with ED data ($\bigcirc$) and RPA results (dotted). The inset shows the 2D inverse zero-field susceptibility.

$$a = \begin{cases} 1.088 \\ 1.486 \end{cases} \quad \text{and} \quad \gamma = \begin{cases} 0.739; & \text{1D} \\ 0.620; & \text{2D}. \end{cases} \quad (27)$$

The ED results for T_m^χ (for clarity, the fit of the ED data is not drawn) deviate only slightly from Eq. (26); in the 1D (2D) model we obtain $a = 1.051$ (1.460) and $\gamma = 0.765$ (0.643). Considering the power-law behavior in the low-field region, the numerically most reliable data are provided by the Bethe-ansatz solution. For the 1D system at $h \leq 0.1$, the Bethe-ansatz results are described by Eq. (26) with

$$a = 0.765 \quad \text{and} \quad \gamma = 0.576. \quad (28)$$

Comparing our results for the 1D model with Ref. 15 ($\gamma \simeq 0.7$), the γ values are in rough agreement, whereas the absolute values of T_m^χ found in Ref. 15 exceed our results by a factor of about 2.5. The dependence of the maximum position on the dimensionality could be used for the interpretation of experimental data.

Our results for the maximum value $\chi_s(T_m^\chi)$ as a function of h in the same field region as before are plotted in Fig. 5(b). Again, they may be described by power laws for $h > 0.2$ (0.6) in the 1D (2D) model. From the Green-function theory we obtain

$$\chi_S(T_m^\chi) = bh^\beta \quad (29)$$

with

$$b = \begin{cases} 0.202 \\ 0.185 \end{cases} \quad \text{and} \quad \beta = \begin{cases} -0.951; & \text{1D} \\ -0.914; & \text{2D}. \end{cases} \quad (30)$$

The ED results for the 1D (2D) model are given by $b = 0.206$ (0.191) and $\beta = -0.964$ (-0.935). At low fields we consider, as above, only the Bethe-ansatz solution for the 1D model which, at $h \leq 0.1$, yields Eq. (29) with

$$b = 0.208 \quad \text{and} \quad \beta = -0.952. \quad (31)$$

Note the remarkable agreement of the Bethe-ansatz results for the field dependence of the maximum height with the findings of the theory and the ED data.
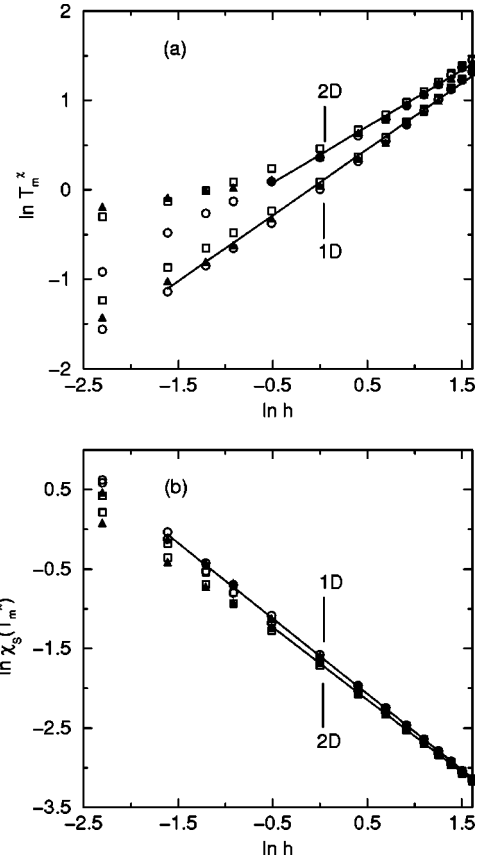

FIG. 5. Logarithmic plot of the field dependence of the position (a) and height (b) of the susceptibility maximum obtained by the Green-function theory ($\blacktriangle$) and fit to a linear dependence (solid) in comparison with ED ($\bigcirc$) and RPA results ($\square$).

The results obtained for the exponent β strongly deviate from the β value of Landau's theory, $\beta = -2/3$. Moreover, we get $m(T_m^\chi) \simeq \text{const.}$ ($\langle S^z \rangle(T_m^\chi) \simeq 0.3$) which also contradicts the law $m(T_m^\chi) \propto h^{1/3}$. This reflects the fact that Landau's theory does not hold for 1D and 2D isotropic ferromagnets, but is valid only on the assumption of a finite critical temperature at $h = 0$ which, however, is not realized in the 1D and 2D systems. Therefore, the approximate agreement of the obtained γ exponents with $\gamma = 2/3$ seems to be accidental.

C. Specific heat

First let us consider the NN spin correlation functions entering the internal energy [cf. Eq. (22)], which are depicted for the 1D and 2D cases in Figs. 6 and 7, respectively. In the 1D model we obtain a very good agreement with the ED data. On the contrary, the RPA results are unsatisfactory; in particular, the longitudinal correlators at low fields and temperatures, obtained from the exact representation of the internal energy, Eq. (22), are negative being incompatible with the ferromagnetic SRO. In the 2D model at low fields, we ascribe the deviations of our analytical curves from the ED data to finite-size effects; in this respect, C_{10}^{zz} may be considered in analogy to $\langle S^z \rangle$ [Fig. 1(b)].
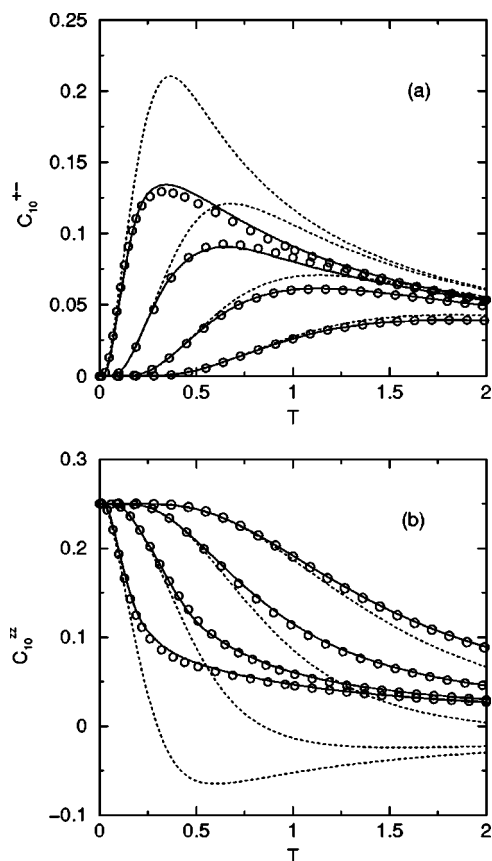
FIG. 6. Nearest-neighbor transverse (a) and longitudinal (b) spin correlation functions of the 1D ferromagnet at the fields $h=0.1$, 0.4, 1.0, and 2.0, from left to right. The Green-function theory (solid) is compared with ED ($\bigcirc$) and RPA results (dotted).
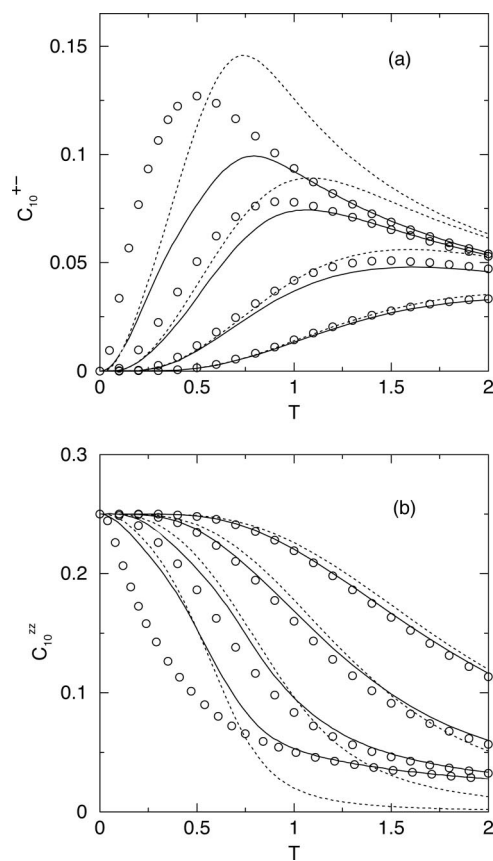

FIG. 7. Nearest-neighbor transverse (a) and longitudinal (b) spin correlation functions of the 2D ferromagnet at the fields $h=0.1$, 0.4, 1.0, and 2.0, from left to right. The Green-function theory (solid) is compared with ED ($\bigcirc$) and RPA results (dotted).

Figure 8 displays the specific heat $C=\partial u/\partial T$ for the 1D ferromagnet. At $h=0$, the temperature dependence of the specific heat exhibits a broad maximum, where the value of the maximum position resulting from the Green-function theory, $T_m^C(h=0)\simeq0.45$, agrees reasonably well with the exact result $T_m^C(h=0)\simeq0.35$ obtained by the Bethe-ansatz and ED methods. Comparing our ED data at $h=0$ with those of Ref. 25 agreeing with the Bethe-ansatz results, the additional weak maximum at $T\simeq0.1$ has to be ascribed to finite-size effects. The broad maximum and the strong decrease of the zero-field specific heat at low temperatures is qualitatively reproduced by the Green-function theory, as already shown in Ref. 22. At very low magnetic fields, besides the high-temperature maximum, a second maximum at low temperatures develops which has not been reported before. The occurrence of two maxima in the specific heat is indicated by our theory, however, at too high fields ($0.03\lesssim h\lesssim0.07$). In a detailed Bethe-ansatz analysis, two maxima in the specific heat are found in the field region $0<h\lesssim0.008$ [see inset of Fig. 8(a)]. At $h\gtrsim0.008$, only one maximum appears. Considering the low-temperature maximum at $h\lesssim0.01$, the position $T_{m,1}^C$ and height $C(T_{m,1}^C)$ are given by the power laws

$$T_{m,1}^C=0.596h^{0.542}, \quad C(T_{m,1}^C)=0.513h^{0.228}. \quad (32)$$

Note that the exponent of $T_{m,1}^C$ nearly agrees with that of T_m^χ given by Eqs. (26) and (28). From the low-field specific heat

it becomes evident again that our theory provides an improved description of SRO, as compared with RPA [cf. Fig. 8(b)] which does not yield a double maximum.

The specific heat for the 2D model is plotted in Fig. 9. We get a good agreement with the ED results, in particular, as the position and height of the maximum is concerned. Note that the small low-temperature bump in the ED data for $h=0.1$ is a finite-size effect. The RPA curves at low fields exhibit a too large maximum height which we ascribe to a poor description of SRO in RPA (see also Fig. 7).

In the 1D and 2D systems at the fields $h>0.4$ and $h>0.1$, respectively, the position of the specific-heat maximum obtained by the Green-function theory may be described by the linear law

$$T_m^C=ah+b \quad (33)$$

with

$$a=\begin{cases}0.433\\0.463\end{cases} \quad \text{and} \quad b=\begin{cases}0.310; & 1D\\0.685; & 2D.\end{cases} \quad (34)$$

IV. SUMMARY

In this paper we developed a Green-function theory of the 1D and 2D $S=1/2$ Heisenberg ferromagnet in a magnetic
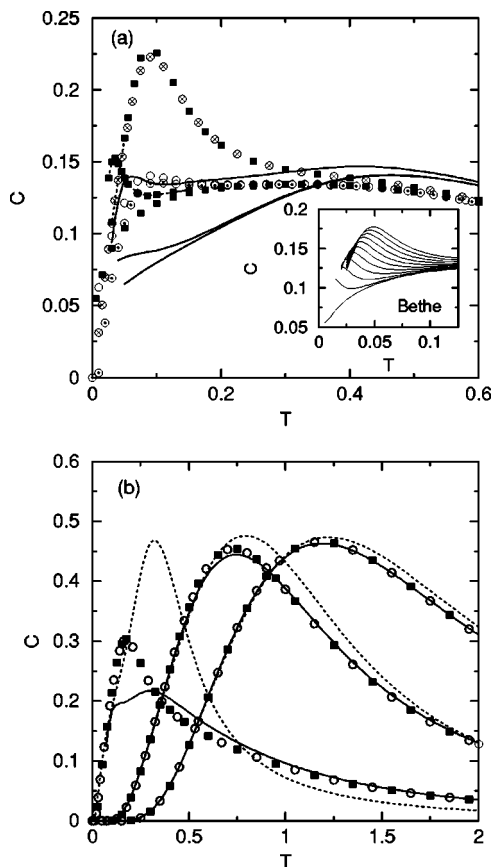
FIG. 8. Specific heat of the 1D ferromagnet obtained by the Green-function (solid) and Bethe-ansatz method (■) at low fields (a), $h=0$, 0.005, and 0.03, from bottom to top, with the ED data denoted by ⊙, ○, and ⊗, respectively, and at higher fields (b), $h=0.1$, 1.0, and 2.0, from left to right, in comparison with ED (○) and RPA results (dotted). For clarity, the Bethe-ansatz data for $h=0.005$ and 0.03 at low temperatures are joined by dotted lines. For low fields the RPA data are not drawn because of the too high maximum [cf. (b)]. The inset exhibits the Bethe-ansatz results for very low fields, $h=0$ to 0.01 in steps of 0.001, from bottom to top.

field which goes one step further than the RPA. The theory allows for the calculation of both transverse and longitudinal spin correlation functions and provides an improved description of magnetic short-range order and of the thermodynamics. Additionally, we performed exact finite-lattice diagonalizations on an $N=16$ chain and a 4×4 square lattice and
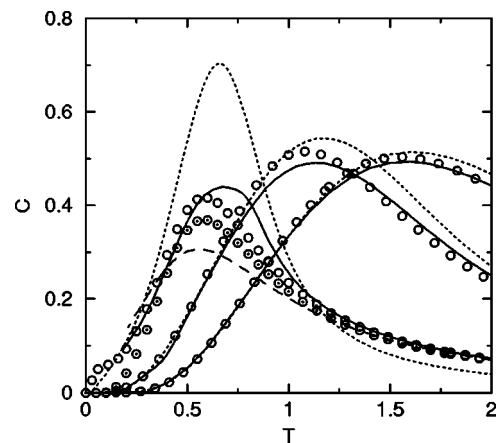

FIG. 9. Specific heat of the 2D ferromagnet at $h=0.1$, 1.0, and 2.0, from left to right, showing the Green-function (solid), ED (○), and the RPA results (dotted). At $h=0$ the Green-function theory (dashed) is compared with ED data (⊙).

obtained exact Bethe-ansatz results for the Heisenberg chain from an eigenvalue analysis of the quantum transfer matrix. Stimulated by recent disscussions we analyzed the field dependence of the maximum in the temperature dependence of the isothermal magnetic susceptibility. We found power laws for the position and height of the susceptibility maximum which are shown not to be related to the predictions of Landau's theory. Paying particular attention to the specific heat of the Heisenberg chain, in a detailed Bethe-ansatz analysis the existence of two maxima in the temperature dependence of the specific heat at very low magnetic fields was proven. The field dependences of the position and height of the low-temperature maximum obey power laws. Altogether, we analyzed the effects of dimensionality (1D versus 2D) on all thermodynamic quantities which may be relevant for the comparison with experiments.

[1] M. J. Manfra, E. H. Aifer, B. B. Goldberg, D. A. Broido, L. Pfeiffer, and K. West, Phys. Rev. B **54**, R17 327 (1996).

[2] N. Read and S. Sachdev, Phys. Rev. Lett. **75**, 3509 (1995).

[3] C. Timm, S. M. Girvin, P. Henelius, and A. W. Sandvik, Phys. Rev. B **58**, 1464 (1998).

[4] P. Henelius, A. W. Sandvik, C. Timm, and S. M. Girvin, Phys. Rev. B **61**, 364 (2000).

[5] S. Feldkemper, W. Weber, J. Schulenburg, and J. Richter, Phys. Rev. B **52**, 313 (1995).

[6] H. Manaka, T. Koide, T. Shidara, and I. Yamada, Phys. Rev. B **68**, 184412 (2003).

[7] S. Feldkemper and W. Weber, Phys. Rev. B **57**, 7755 (1998).

[8] M. Takahashi, P. Turek, Y. Nakazawa, M. Tamura, K. Nozawa, D. Shiomi, M. Ishikawa, and M. Kinoshita, Phys. Rev. Lett. **67**, 746 (1991).

[9] C. P. Landee and R. D. Willett, Phys. Rev. Lett. **43**, 463 (1979).

[10] A. Ecker, P. Fröbrich, P. J. Jensen, and P. J. Kuntz, J. Phys.: Condens. Matter **11**, 1557 (1999).

[11] S. V. Tjablikov, *Methods in the Quantum Theory of Magnetism* (Plenum Press, New York, 1967).

[12] H. B. Callen, Phys. Rev. **130**, 890 (1963).

[13] M. Yamada and M. Takahashi, J. Phys. Soc. Jpn. **55**, 2024 (1986).

[14] M. Takahashi, Phys. Rev. B **44**, 12382 (1991); H. Nakamura and M. Takahashi, J. Phys. Soc. Jpn. **63**, 2563 (1994).

[15] J. Sznajd, Phys. Rev. B **64**, 052401 (2001).

[16] S. Winterfeldt and D. Ihle, Phys. Rev. B **56**, 5535 (1997); **59**, 6010 (1999).

[17] C. Schindelin, H. Fehske, H. Büttner, and D. Ihle, Phys. Rev. B **62**, 12 141 (2000); D. Ihle, C. Schindelin, and H. Fehske, *ibid.* **64**, 054419 (2001).

[18] A. Klümper, Eur. Phys. J. B **5**, 677 (1998).

[19] J. Suzuki, J. Phys. A **32**, 2341 (1999).

[20] H. Shimahara and S. Takada, J. Phys. Soc. Jpn. **60**, 2394 (1991); **61**, 989 (1992).

[21] K. Elk and W. Gasser, *Die Methode der Greenschen Funktionen in der Festkörperphysik* (Akademie-Verlag, Berlin, 1979); W. Nolting, *Quantentheorie des Magnetismus*, Vol. 2 (B. G. Teubner, Stuttgart, 1986).

[22] J. Kondo and K. Yamaji, Prog. Theor. Phys. **47**, 807 (1972); K. Yamaji and J. Kondo, Phys. Lett. **45A**, 317 (1973).

[23] D. A. Yablonskiy, Phys. Rev. B **44**, 4467 (1991).

[24] V. Markovich, E. Rozenberg, G. Gorodetsky, B. Revzin, J. Pelleg, and I. Felner, Phys. Rev. B **62**, 14 186 (2000).

[25] J. C. Bonner and M. E. Fisher, Phys. Rev. **135**, A640 (1964).